Visco-Rubber Elastic Model for Pressure Sensitive Adhesive

Kazuhisa Maeda†, Shigenobu Okazawa*, Koji Nishigichi* and Takashi Iwamoto*

Abstract— **A material model to describe large deformation of pressure sensitive adhesive (PSA) is presented. A relationship between stress and strain of PSA includes viscoelasticity and rubber-elasticity. Therefore, we propose the material model for describing viscoelasticity and rubber-elasticity and formulate rate form of the presented material model for three dimensional finite element analysis. And we validate the present formulation by using one axis tensile calculation.**

Keywords: viscoelasticity, rubber-elasticity, adhesive, large deformation, finite element method

1 Introduction

The elastic modulus of a pressure sensitive adhesive (PSA) is about 10^5Pa at room temperature and indicates extremely low compared with other solid materials. Therefore, large deformation behavior can be observed in conventional PSA deformation.

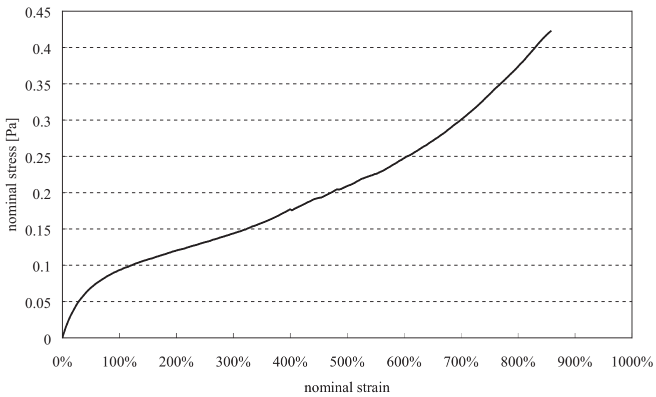

Figure 1: Stress-strain curve of PSA

Fig.1 shows the tensile Stress-Strain curve of PSA. As shown in Fig.1, the stress increases exponentially for large strain zone. This behavior is called "rubber-elasticity" in this paper. PSA is generally considered to be a viscoelastic material. However, only viscoelasticity can not describe practical behavior including rubber-elasticity of PSA consisitently.

The generalized Maxwell model is usually used for describing viscoelasticity. On the other hands, hyperelasticity is popular to simulate increase in stress[1]. However, there is a difficulty in use of hyperelasticity, because hyperelasticity independ on time. In order to evaluate material constants, hyperelasticity needs time independent parameters with experimental data without stress relaxation. The aim of this study is the establishment of material model describing visco and rubber elasticity for PSA . The established material model can indicate rubber-elasticity without hyperelastic model. We formulate the above material model and its rate formulation for finite element analysis and then shows the validation by using computational example.

2 Material Model

2.1 Concept of Proposed Material Model

PSA indicates remarkable viscoelasticity at room temperature. The generalized Maxwell model for describing viscoelasticity is used in the present study. Fig.2 shows generalized Maxwell model. Where i denotes unit number of the generalized Maxwell model. And E and η are elastic modulus of spring and viscous coefficient of dashpot, respectively.

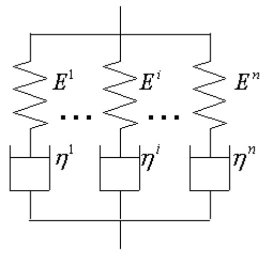

Figure 2: Generalized Maxwell model

However, the generalized Maxwell model of Fig.2 can not describe rubber-elastic behavior of PSA as shown in Fig.1. The reason is that elastic modulus of the generalized Maxwell model is constant. Then, we propose evaluation of elastic modulus of the spring component. Fig.3

†Nitto Denko Corporation, Department of Reliability Evaluation Technology, Toyohashi, Aichi, 441-3194, Japan, Tel/Fax: +81-532-41-8849/43-1853 Email: kazuhisa_maeda@gg.nitto.co.jp

*Hiroshima University, Department of Social and Environmental Engineering, Higashi-Hiroshima, Hiroshima 739-8527, Japan, Tel/Fax: +81-82-424-7810/422-7194, Email: okazawa@hiroshima-u.ac.jp (Shigenobu Okazawa)

ISBN: 978-988-17012-8-2
ISSN: 2078-0958 (Print); ISSN: 2078-0966 (Online)

shows the modified generalized Maxwell model. This proposed model is called "Advanced Generalized Maxwell Model". In the advanced generalized Maxwell model, elastic modulus is function of total strain. In addition, viscous coefficients of dashpot is function of strain to assume that relaxation time is constant like the generalized Maxwell model.

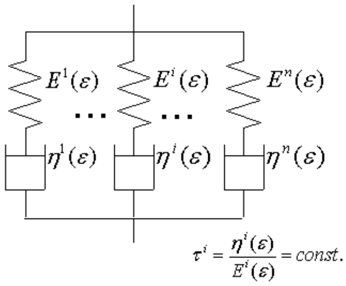

Figure 3: Advanced Generalized Maxwell model

2.2 Rubber-Elasticity

Elastic moduli for the advanced generalized Maxwell model are determined as the function of total strain. First, we measure stress relaxation behavior with various initial strains in order to investigate the strain dependency of an elastic modulus. For this experiment, common acrylic PSA is used. Cylindrical PSA sample, whose cross-section is 2mm^2, is attached to a tensile machine so that the length of PSA is 10mm, and initial strain is given 100% by nominal strain. Then, the sample is extended and keeps in the fixed strain. The stress relaxation curve is obtained by measuring the stress change at the measurement time. The relation of nominal stress - nominal strain is changed into the relation of true stress - true strain. Regression analysis is applied to the obtained curve using the stress relaxation formula of the generalized Maxwell model as shown in eq.(1), and we get the 5 sets of relaxation time, τ^i, and elastic modulus of the spring component, E^i.

$$\sigma = \sum_{i=1}^{n} E^i \exp(-\frac{t}{\tau^i}) \tag{1}$$

where σ, E, τ, and i denote true stress, elastic modulus of a spring component, relaxation time, and the unit number respectively. Then, the stress relaxation measurement with initial strain 200, 300, 400, 500, and 600% is measured, and we get the sets of the relaxation time and elastic modulus at each initial strain.

Table.1 shows relaxation times and elastic moduli of each strain. The strains in Table.1 are converted into true strain. Then, elastic modulus E is depends on the total strain and is considered about each case of τ. The case of $\tau = 100[sec]$ is considered for an example. Fig.4 shows elastic modulus, which depends on strain.

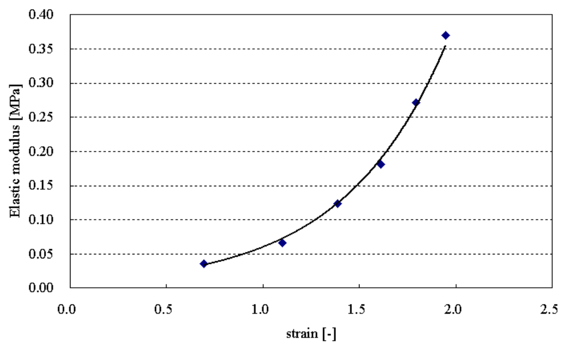

Figure 4: Relationship between elastic modulus and strain

When the exponential function of strain is used as an approximated curve to this curve, the correlation coefficient is very high. This is the same for the cases of other relaxation times. So, we decide to use the exponential function of strain as a function of an elastic modulus as follows.

$$E^i = A^i \exp(B^i \varepsilon) \tag{2}$$

where A and B denotes material parameter, and ε does strain.

3 Constitutive Formulation

Although the elastic modulus of the spring component of the advanced model is defined by eq.(2), it is necessary to distinguish scalar, vector, and tensor strictly in the case of dealing with three dimensions. So, the elastic modulus of a spring component is replaced with eq.(3). Here, an elastic modulus uses shear elastic modulus G.

$$G^i = A^i \exp(B^i \hat{\varepsilon}) \tag{3}$$

where $\hat{\varepsilon}$ denotes scalar of strain. And $\hat{\varepsilon}$ is defined by eq.(4) using the small strain tensor, $\boldsymbol{\varepsilon}$.

$$\hat{\varepsilon} = \sqrt{\frac{2}{3}\boldsymbol{\varepsilon} : \boldsymbol{\varepsilon}} \tag{4}$$

It is assumed that viscoelasticity is in a deviatoric component in the model. So, a constitutive equation of deviatoric and volumetric component is respectively formulated, and then the constitutive equation of whole component is formulated.

3.1 Daviatoric Component

The spring of the ith unit is assumed to be an incompressible linear elastic material. Here shear elastic modulus and small strain tensor of the spring of ith unit is expressed as G^i and $\boldsymbol{\varepsilon}^{sp,i}$ respectively, and the deviatoric stress tensor of ith spring unit is

$$\boldsymbol{\sigma}'^i = 2G^i \boldsymbol{\varepsilon}^{sp,i} \tag{5}$$

The prime of a right shoulder shows a deviatoric component. The material time derivative of both sides of eq.(5)

ISBN: 978-988-17012-8-2
ISSN: 2078-0958 (Print); ISSN: 2078-0966 (Online)

Table 1: Relaxation times and elastic moduli of each strain

Relaxation time [s]	True strain					
	0.6931	1.0986	1.3863	1.6094	1.7918	1.9459
1.00×10^0	0.1541	0.3637	0.5694	1.2057	2.0546	3.8663
1.00×10^1	0.0326	0.0832	0.1368	0.3548	0.5107	0.7711
1.00×10^2	0.0363	0.0665	0.1237	0.1808	0.2078	0.3701
1.00×10^3	0.0250	0.0519	0.0761	0.1040	0.1549	0.1522
1.00×10^{10}	0.0639	0.1326	0.2150	0.3279	0.4608	0.5936

gives

$$\frac{D\boldsymbol{\sigma}'^i}{Dt} = 2G\boldsymbol{D}^{sp,i} + \frac{DG^i}{Dt}\frac{\boldsymbol{\sigma}'^i}{G^i} \tag{6}$$

where $\boldsymbol{D}$ denotes rate of strain tensor. The left side of eq.(6) does not have objectivity. So the constitutive equation is not objective. Therefore object stress rate is assumed

$$\left(\frac{D\boldsymbol{\sigma}'^i}{Dt}\right)_{(*)} = 2G\boldsymbol{D}^{sp,i} + \frac{DG^i}{Dt}\frac{\boldsymbol{\sigma}'^i}{G^i} \tag{7}$$

where $(*)$ with the lower right means arbitrary objective stress rate. Eq.(7) is used as a constitutive equation of a spring.

Next, the dashpot of ith unit is considered. The shear viscous coefficient and the strain rate tensor of ith dashpot unit is expressed as η^i and $\boldsymbol{D}^{dp,i}$ respectively. And dashpot is assumed to be incompressible Newtonian fluid. The constitutive equation of ith dashpot unit is given as

$$\boldsymbol{\sigma}'^i = 2\eta^i\boldsymbol{D}^{dp,i} \tag{8}$$

The model property insists that the small strain tensor of ith unit can be assumed to be equal to the strain of the whole model. That is, $\boldsymbol{\varepsilon} = \boldsymbol{\varepsilon}^i = \boldsymbol{\varepsilon}^{sp,i} + \boldsymbol{\varepsilon}^{dp,i}$. The material time derivative of this equation gives

$$\boldsymbol{D} = \boldsymbol{D}^{sp,i} + \boldsymbol{D}^{dp,i} \tag{9}$$

From eqs.(7)(8)(9), the constitutive equation of the ith unit's deviatoric component is derived to

$$\left(\frac{D\boldsymbol{\sigma}'^i}{Dt}\right)_{(*)} = 2G\boldsymbol{D}^{sp,i} + \frac{DG^i}{Dt}\frac{\boldsymbol{\sigma}'^i}{G^i} - \frac{\boldsymbol{\sigma}'^i}{\tau^i} \tag{10}$$

The material time derivative of eq.(3) gives

$$\frac{DG^i}{Dt} = B^iG^i\frac{D\hat{\varepsilon}}{Dt} \tag{11}$$

And eq.(10) is given as, with eq.(11)

$$\left(\frac{D\boldsymbol{\sigma}'^i}{Dt}\right)_{(*)} = 2G\boldsymbol{D}^{sp,i} + B^i\frac{D\hat{\varepsilon}}{Dt}\boldsymbol{\sigma}'^i - \frac{\boldsymbol{\sigma}'^i}{\tau^i} \tag{12}$$

Since the stress of the whole model is derived from summation of the stress of each unit, the constitutive equation of the whole model is described to

$$\left(\frac{D\boldsymbol{\sigma}'^i}{Dt}\right)_{(*)} = \sum_i\left(2G\boldsymbol{D}^{sp,i} + B^i\frac{D\hat{\varepsilon}}{Dt}\boldsymbol{\sigma}'^i - \frac{\boldsymbol{\sigma}'^i}{\tau^i}\right) \tag{13}$$

3.2 Volumetric Component

Here it is assumed that the volumeric component is a compressible linear elastic material. Pressure, p, is given as

$$p = -K_v tr\varepsilon \tag{14}$$

where Kv denotes the coefficient of volumetric elasticity derived from eq.(15).

$$K_v = \frac{\sum_i E^i}{3\left(1-2\nu\right)} \tag{15}$$

where ν denotes Poisson ratio. The material time derivative of eq.(14) gives

$$\frac{Dp}{Dt} = \frac{DK_v}{Dt}\frac{p}{K_v} - K_v tr\boldsymbol{D} \tag{16}$$

where

$$K_v = \frac{2\left(1+\nu\right)}{3\left(1-2\nu\right)}\sum_i G^i \tag{17}$$

$$\frac{DK_v}{Dt} = \frac{2\left(1+\nu\right)}{3\left(1-2\nu\right)}\sum_i \frac{DG^i}{Dt} \tag{18}$$

Substituting eq.(11) into eq.(18) derives to

$$\frac{DK_v}{Dt} = \frac{2\left(1+\nu\right)}{3\left(1-2\nu\right)}\sum_i B^iG^i\frac{D\hat{\varepsilon}}{Dt} \tag{19}$$

Therefore, the constitutive equation of volumetric component is

$$\frac{Dp}{Dt} = p\frac{D\hat{\varepsilon}}{Dt}\frac{\sum_i B^iG^i}{\sum_i G^i} - K_v tr\boldsymbol{D} \tag{20}$$

3.3 Whole Component

Here the Jaumann rate is used as objective stress rate. The material time derivative of Cauchy stress and its Jaumann rate are connected with eq.(21).

$$\left(\frac{D\boldsymbol{\sigma}}{Dt}\right)_{(J)} = \frac{D\boldsymbol{\sigma}}{Dt} + \boldsymbol{W}\cdot\boldsymbol{\sigma} - \boldsymbol{\sigma}\cdot\boldsymbol{W} \tag{21}$$

where $\boldsymbol{W}$ denotes spin tensor, and the lower right (J) shows the Jaumann rate. Here the Cauchy stress is divided into deviatoric and volumetric component,

$$\boldsymbol{\sigma} = \boldsymbol{\sigma}' - p\boldsymbol{I} \tag{22}$$

ISBN: 978-988-17012-8-2
ISSN: 2078-0958 (Print); ISSN: 2078-0966 (Online)

where $\boldsymbol{I}$ denotes unit tensor. Substituting eq.(22) into eq.(21) derives to

$$\left(\frac{D\boldsymbol{\sigma}}{Dt}\right)_{(J)} = \left(\frac{D\boldsymbol{\sigma}'}{Dt}\right)_{(J)} - \frac{Dp}{Dt}\boldsymbol{I} \tag{23}$$

Therefore, substituting constitutive equation of deviatoric and volumetric component into eq.(23), the constitutive equation of the whole component is derived to

$$\begin{aligned}\left(\frac{D\boldsymbol{\sigma}}{Dt}\right)_{(J)} &= \sum_i \left(2G^i\boldsymbol{D} + B^i\frac{D\hat{\varepsilon}}{Dt}\boldsymbol{\sigma}'^i - \frac{\boldsymbol{\sigma}'^i}{\tau^i}\right) \\ &- \left(p\frac{D\hat{\varepsilon}}{Dt}\frac{\sum_i B^iG^i}{\sum_i G^i} - K_v tr\boldsymbol{D}\right)\boldsymbol{I}\end{aligned} \tag{24}$$

4 Explicit Finite Element Method

The present study employs an explicit finite element method[2] to calculate the following computational example. The explicit finite element method is computationally robust because of no iterations.

4.1 Discrete equilibrium equation

The equilibrium equation ignoring the body force is,

$$\rho\boldsymbol{a} = \frac{\partial\boldsymbol{\sigma}}{\partial\boldsymbol{x}} \tag{25}$$

where ρ is the material density, $\boldsymbol{a}$ is the spatial acceleration, and $\boldsymbol{\sigma}$ is the Cauchy stress.

We can derive the virtual work equation by multiplying both sides of eq.(25) by the arbitrary virtual displacement $\delta\boldsymbol{u}$ with the Gauss' divergence theorem of volume V.

$$\int_V \rho\boldsymbol{a}\cdot\delta\boldsymbol{u}dV + \int_V \boldsymbol{\sigma} : (\delta\boldsymbol{\varepsilon})dV = \int_{\partial V} \bar{\boldsymbol{t}}\cdot\delta\boldsymbol{u}dS \tag{26}$$

where $\bar{\boldsymbol{t}}$ is the external surface force on the boundary area ∂V, and $\boldsymbol{\varepsilon}$ is the linear strain as follows,

$$\boldsymbol{\varepsilon} = \frac{1}{2}\left[\left(\frac{\partial\boldsymbol{u}}{\partial\boldsymbol{x}}\right) + \left(\frac{\partial\boldsymbol{u}}{\partial\boldsymbol{x}}\right)^T\right] \tag{27}$$

The discrete equilibrium equation can be derived using the finite element as follows;

$$\boldsymbol{M}\boldsymbol{a} + \boldsymbol{F}_{int} = \boldsymbol{F}_{ext} \tag{28}$$

where $\boldsymbol{M}$ is the mass matrix, $\boldsymbol{F}_{int}$ and $\boldsymbol{F}_{ext}$ are the internal and external force vectors respectively. For the numerical integration of the isoparametric element in the plane strain state, the selective reduced integration method is used to avoid volumetric locking [3].

4.2 Central difference method

To advance the time of the discrete equilibrium eq.(28), we select the central difference method. Let Δt is the time increment from time t^n to t^{n+1}. The current time is t^n and any properties of the material at time t^{n+1} will be explicitly calculated with the central difference method. The material coordinates $\boldsymbol{x}$ at t^{n+1} is evaluated with the material velocity $\boldsymbol{v}$ at the central incremental time $t^{n+\frac{1}{2}}$.

$$\boldsymbol{x}^{n+1} = \boldsymbol{x}^n + \boldsymbol{v}^{n+\frac{1}{2}}\Delta t \tag{29}$$

where the material velocity $\boldsymbol{v}$ at time $t^{n+\frac{1}{2}}$ is

$$\boldsymbol{v}^{n+\frac{1}{2}} = \boldsymbol{v}^{n-\frac{1}{2}} + \boldsymbol{a}^n\Delta t \tag{30}$$

and the spatial acceleration $\boldsymbol{a}$ at time t^n is solved as follows with eq.(28).

$$\boldsymbol{a}^n = \boldsymbol{M}^{-1}(\boldsymbol{F}^n_{ext} - \boldsymbol{F}^n_{int}) \tag{31}$$

Eq.(31) requires no solution of the simultaneous equations by using the diagonal lumped mass matrix for $\boldsymbol{M}$.

5 Computational Results

Here, in order to verify an above-mentioned technique, one axis tensile measurement of PSA is analyzed.

5.1 Material Constants

The material constants which must be defined in the constitutive equation are A^i, B^i and τ^i. These values are calculated from the experimental data of one axis elongation measurement.

First, the method of one axis elongation measurement is explained. It is measured at room temperature. Cylindrical PSA sample whose cross-section is 2mm^2 is attached to the tensile machine so that the length of PSA is 10mm, the sample is elongated at the predetermined rate. The rate is 10, 50, 300 mm/min. Since the data from the measurement gives nominal stress and nominal strain, the Stress-Strain curve changes into true stress - true strain is made.

Constitutive equation of the advanced model calculated by one dimension is

$$\frac{d\sigma}{dt} = \sum A^i \exp\left(B^i\varepsilon\right)\frac{d\varepsilon}{dt} - \sum\left(\frac{1}{\tau^i} - B^i\frac{d\varepsilon}{dt}\right)\sigma^i \tag{32}$$

Eq.(32) is applied to the Stress-Strain curve with nonlinear least squares method, and the material constants are determined. Approximate curve is calculated so that all Stress-Strain curve with different three elongation rate are satisfied. The result is shown in Table.2.

5.2 Comparison with Experiment

Analysis model is shown in Fig.5. The analysis object is cubic PSA whose length of one side is 1cm. The density of PSA uses 1000kg/m^3.

ISBN: 978-988-17012-8-2
ISSN: 2078-0958 (Print); ISSN: 2078-0966 (Online)

Table 2: Material constants

Relaxation times [s]	A^i [Pa]	B^i
1.00×10^0	1.28×10^5	1.17
1.00×10^1	8.93×10^1	4.40
1.00×10^2	3.71×10^2	3.67
1.00×10^3	1.30×10^5	0.67
1.00×10^6	7.13×10^1	3.85

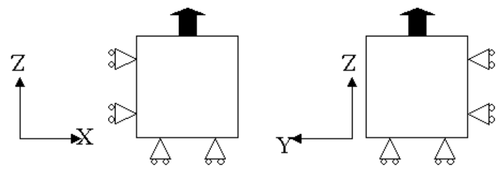

Figure 5: Boundary conditions

The analysis is calculated with one element model for the efficiency of analysis time. PSA shows near incompressibility. However, the analysis using 0.49 for the Poisson ratio is stopped before completing calculation. The reason is considered to be locking. Since the purpose was verification of the model this time, 0.3 is used as Poisson ratio. The elongation rate used for analysis is 5, 50, and 500 mm/min. The material constants use the values shown in Table.2.

The result is shown in Fig.6. In Fig.6, the rate, for example 5mm/min, shows elongating rate. Fig.6 shows that the computational result can describe the experimental data well. And it shows that the elongating rate dependability originating in the viscoelasticity can be described well. Therefore, it is thought that this model is appropriate as a material model describing deformation of PSA.

However, some difference between computational result and experimental data can be observed in the area of large strain and at high elongating rate. It is thought that the reason for this difference is using 0.3 for Poisson ratio.

5.3 Investigation of Poisson Ratio

In order to study the reason for bad correlation at high elongating rate, we analyze at various Poisson ratio. The result is shown in Fig.7. Fig.7 is the result of the analysis at 500mm/min of elongating rate and the area of nominal strain 400-600% is magnified.

The correlation between computational result and experimental data is so good that the Poisson ratio used for calculation is close to 0.5. The curve of the Poisson ratio 0.4 shows the strange behavior near 550% of nominal strain. This is because the analysis does not progress according to the locking phenomenon.

From above mentioned, it is thought that the reason why the correlation worsens at the area of large strain is to estimate the Poisson ratio to be low, and that good correlation is acquired if the near incompressibility can be described.

6 Conclusions and Future Work

This paper has treated the material model which can describe the deformation of PSA. Our results indicate the following.

1. The present advanced generalized Maxwell model can describe visco and rubber elasticity.
2. We have formulized the three-dimensional constitutive equation of the advanced generalized Maxwell model.
3. We have validated the proposed advanced generalized Maxwell model with the one axis tensile analysis.

The remained subjects to simulate practical PSA behavior with large deformation are as follows.

1. The present code uses dynamic explicit method. Therefore, computational time step size is extremely small because of the requirement of the Courant condition. It is necessary to consider the solution method, which can use large time step size, for suitable analysis of PSA deformation.
2. The highly distorted Lagrangian finite elements cannot retain numerical accuracy. The present formulation should be extended to an Eulerian formulation[4], which is attractive for large deformation problem like PSA.

References

[1] Simo, J.C. and Hughes, T.J.R., *Computational Inelasticity*, Springer, 1973.

[2] Okazawa, S., Kashiyama, K. and Kaneko, K., "Large deformation dynamic solid analysis by Eulerian solution based on stabilized finite element method", *International Journal for Numerical Methods in Engineering*, 72, pp.1544–1559, 2007.

[3] Hughes, T.J.R. "Generalization of selective integration procedures to anisotropic and nonlinear media". *International Journal for Numerical Methods in Engineering*, 15, pp.1413–1418, 1980.

[4] Benson, D.J., Okazawa, S., "Contact in a multimaterial Eulerian finite element formulation," *Computer Methods in Applied Mechanics and Engineering*, 193, pp. 4277-4295, 2004.

ISBN: 978-988-17012-8-2
ISSN: 2078-0958 (Print); ISSN: 2078-0966 (Online)

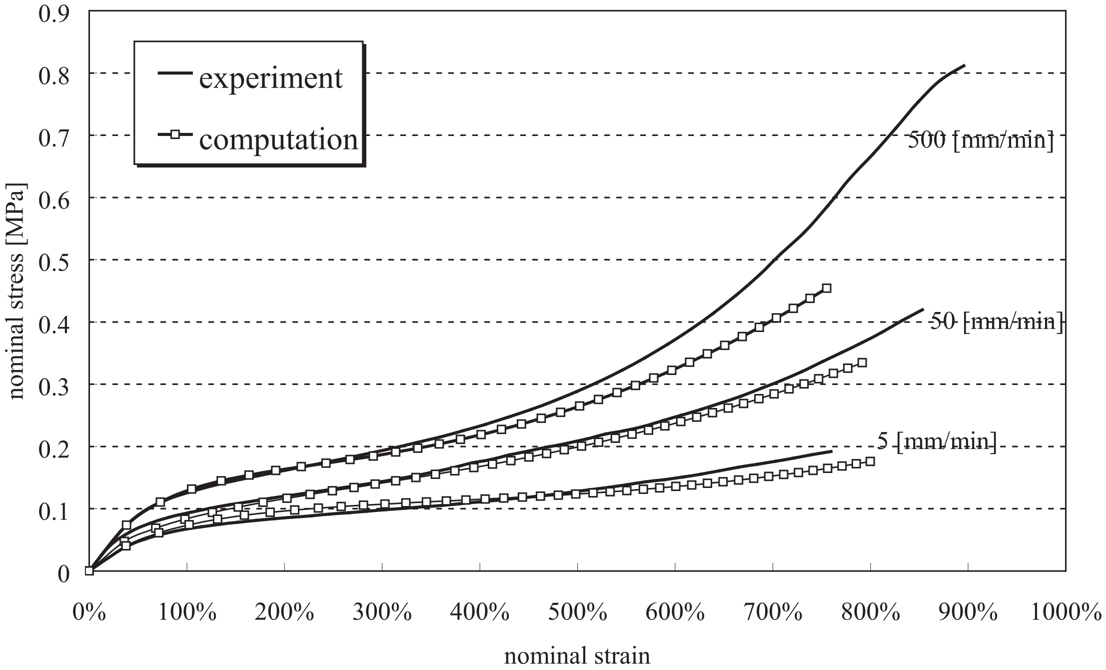

Figure 6: Computational and experimental stress-strain curves

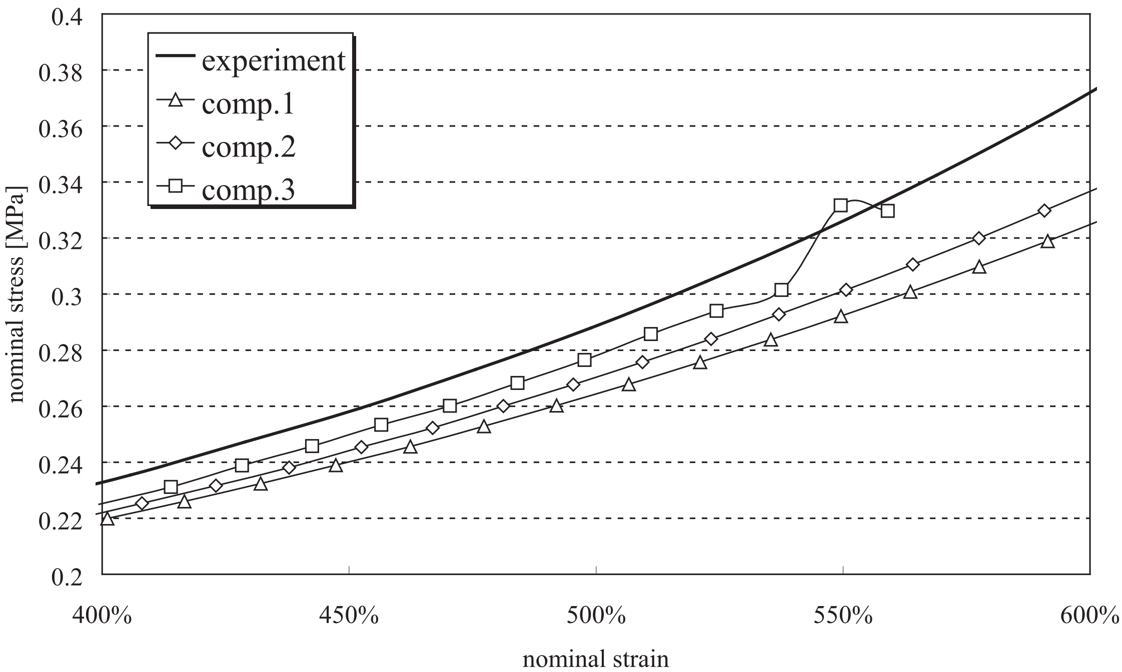

Figure 7: Stress-strain curves with different Poisson ratios. Comp.1, 2 and 3 are computational solutions in case of Poisson ratio 0.3, 0.35 and 0.4 respectively.

ISBN: 978-988-17012-8-2
ISSN: 2078-0958 (Print); ISSN: 2078-0966 (Online)